

Spontaneous polarization and piezoelectric field in GaN/Al_{0.15}Ga_{0.85}N quantum wells: Impact on the optical spectra

R. Cingolani,* A. Botchkarev, H. Tang,[†] and H. Morkoç
Virginia Commonwealth University, Richmond, Virginia 23173

G. Traetta, G. Coli,[‡] and M. Lomascolo[§]

Istituto Nazionale Fisica della Materia (INFN), Dipartimento Ingegneria dell'Innovazione, University of Lecce, 73100 Lecce, Italy

A. Di Carlo, F. Della Sala, and P. Lugli

Istituto Nazionale Fisica della Materia (INFN) -Department of Electronic Engineering, University "Tor Vergata," 00133 Rome, Italy

(Received 16 November 1998; revised manuscript received 21 July 1999)

We have investigated the effects of the built-in electric field in GaN/Al_{0.15}Ga_{0.85}N quantum wells by photoluminescence spectroscopy. The fundamental electron heavy-hole transition redshifts *well below* the GaN bulk gap for well widths larger than 3 nm for the specific quantum wells investigated and exhibits a concomitant reduction of the intensity with increasing well thickness. The experimental data are quantitatively explained by means of a self-consistent tight-binding model that includes screening (either dielectric or by free-carriers), piezoelectric field and spontaneous polarization field. The impact of the built-in field on the exciton stability is discussed in detail. We demonstrate that the exciton binding energy is substantially reduced by the built-in field, well below the values expected from the quantum size effect in the flat band condition.

I. INTRODUCTION

A sizable redshift of the ground-level transition of GaN/Al_{0.15}Ga_{0.85}N and In_xGa_{1-x}N/GaN quantum wells has been observed by various groups with increasing the well width in the range 1–10 nm.^{1–6} This phenomenon is sometimes accompanied by the concomitant reduction of the oscillator strength and by the increase of the characteristic decay time of the emission. All together, these effects point towards the existence of a strong built-in electric field in the heterostructures, which causes a substantial quantum confined Stark effect. The early interpretation for such a Stark effect was that it was caused by the strain induced piezoelectric field.^{1–5} However, very recently the important role of the spontaneous polarization charge accumulated at the GaN/Al_{0.15}Ga_{0.85}N interfaces has been pointed out by the experimental work of Ref. 6, where the anomalous well width dependence of the ground-level transition was deduced by reflectance studies, following the pioneering theoretical work of Refs. 7–9.

In this paper, we have investigated in detail the effects of the built-in field on the luminescence spectra of GaN/Al_{0.15}Ga_{0.85}N quantum wells. The quantitative analysis of the red-shift and oscillator strength of the emission is performed by means of a self-consistent tight-binding (TB) model, which specifically accounts for the total built-in field (given by the piezoelectric and spontaneous polarization terms) and for the screening, either dielectric or induced by the photogenerated carriers. We find that a total built in field of the order of MV/cm, originating primarily from the spontaneous polarization charge formed at the GaN/Al_{0.15}Ga_{0.85}N interfaces with a minor contribution from the piezoelectric field induced by the strain (either lattice mismatch or thermal strain), is needed to explain the optical data. The macroscopic effects of the built-in field are: first, a band bending

and a redshift of the gap, which largely overcome the blue-shift expected from the quantum size effect. This causes the fundamental transition of the quantum wells to occur at energy *well below* the bulk GaN gap for well width larger than 3 nm (for the specific case of GaN/Al_{0.15}Ga_{0.85}N). Second, the built-in field produces a progressive separation of the electron and hole wavefunctions with increasing the well width, resulting in the decrease of the emission strength (and eventually in the increase of the decay time) and in the strong reduction of the exciton binding energy. This latter point is quite relevant in Nitride quantum wells, which would be otherwise expected to form quite stable excitons due to the strong polarity of the crystal. In fact, we demonstrate that the exciton binding energy calculated by using the self-consistent wavefunctions is reduced by a factor 2–3 (depending on the well width) with respect to that evaluated for the square well with flat bands.

II. EXPERIMENT

One- and two-photon absorption photoluminescence spectroscopy have been applied to investigate GaN/Al_{0.15}Ga_{0.85}N quantum wells of increasing thickness. The samples were grown by reactive molecular-beam epitaxy on sapphire substrates. Following a chemical and in situ cleaning of *c*-plane sapphire substrates, a thin AlN buffer layer was grown at 850 °C with ammonia as the active nitrogen source. The AlN layer was followed by the growth of a 1 μm-thick GaN buffer layer grown at 800 °C. Finally, the quantum well region was grown. Each sample consisted of 10 GaN quantum wells. Five samples of well width $L_w = 2, 3, 4, 5,$ and 9 nm, were grown and analyzed. The barrier width and composition were kept constant in all samples (Al_{0.15}Ga_{0.85}N barriers of thickness $L_b = 10$ nm).

Linear luminescence was excited either by the 325-nm

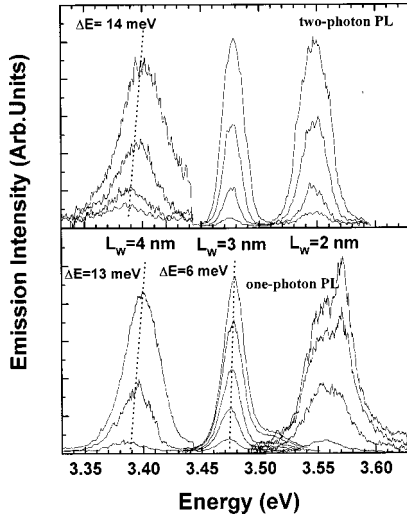


FIG. 1. Two-photon absorption (top) and one-photon absorption (bottom) luminescence spectra recorded at 10 K and for increasing excitation intensities in three different quantum well samples. The linear spectra are recorded in the power range 10 kW/cm^2 – 100 kW/cm^2 . The nonlinear spectra are recorded in the range 300 kW/cm^2 – 1.5 MW/cm^2 , with excitation in the transparency region. The screening induced blueshift (ΔE) is indicated by the dashed lines. The high-energy peak appearing the 2-nm sample at high-pumping intensity is probably due to recombination involving the B valence band.

line of a cw He-Cd laser (10 mW power) or by the 337.1 line of a pulsed N_2 laser (300 kW peak power), in order to get rid of the extrinsic emission bands and to study the density-dependent screening of the built-in field generated by the photogenerated carriers. Two-photon absorption induced luminescence was also measured in order to make sure that the observed blueshift was not due to band filling of hot electron-hole pairs, and to avoid the undesired occurrence of localized states and impurities emission in the spectra. In these experiments the near-half-gap excitation was provided by the tunable output of a pulsed parametric oscillator. All measurements were performed at 10 K.

III. EXPERIMENTAL RESULTS

In Fig. 1, we display a few representative photoluminescence spectra recorded at 10 K under pulsed one- and two-photon absorption excitation and for different power densities. First of all, we note that under pulsed excitation the quantum well emission is dominant over the impurity- and phonon-related emission bands. The E_{1e1h} emission energy decreases with increasing well width, as expected from the quantum size effect. However, we note that for large well widths the E_{1e1h} transition falls *below* the bulk GaN gap (3.51 eV @ 10 K). In order to eliminate possible extrinsic recombination processes, we have performed two-photon absorption experiments with approximately half-gap excitation. Both the linear and nonlinear spectra exhibit the same energy positions and linewidths for the quantum well structures under investigation, indicating that carrier heating or extrinsic effects do not influence the luminescence spectra of these samples. Furthermore, with increasing photogeneration rate all samples exhibit a substantial blue-shift, whose strength

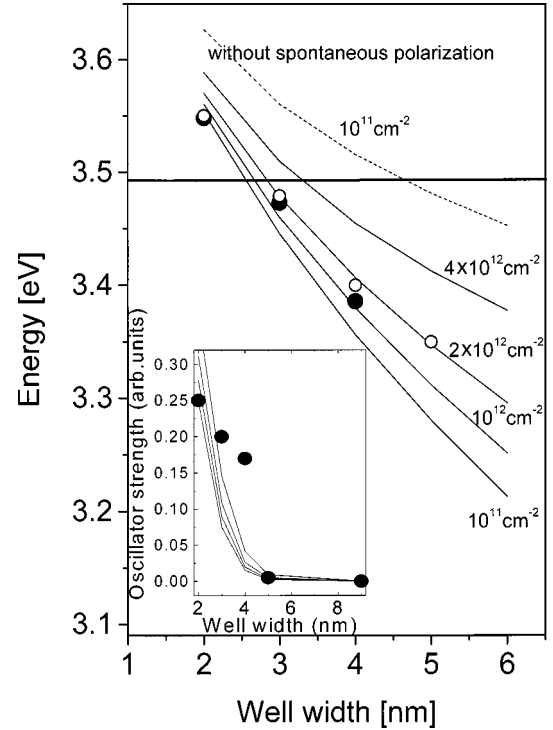


FIG. 2. Well-width dependence of the ground-level emission energy at 10 K. The symbols indicate the measured values (full symbols at low-excitation intensity, empty symbols at high excitation intensity). The emission intensity of the 5-nm sample was reduced dramatically, so that detectable signal could only be observed at high-excitation intensity. The continuous curves are the results of the self-consistent TB model with different photogenerated carrier densities. The dashed curve is the self-consistent TB model neglecting the spontaneous polarization charge. Inset: Measured integrated emission intensity (symbols) and self-consistent calculations for different photogenerated densities (curves calculated for the same densities reported in the figure).

increases in wider wells. This suggests a screening induced blueshift caused by the partial compensation of the Stark effect by the photogenerated carriers. It is important to mention that the emission spectra do not show any significant intensity dependence under low-power cw excitation, suggesting that at low photogeneration rates the screening of the built-in field is negligible. Moreover, the occurrence of localization under low-power cw excitation shown in Ref. 6, which hinders the exact well width dependence and power dependence of the ground-level emission, is avoided by the application of two-photon absorption spectroscopy in our experiments.

In Fig. 2 the symbols display the well-width dependence of the ground-level emission energy at 10 K. The quantum well emission falls below the bulk GaN gap for well widths larger than 3 nm. Furthermore, an abrupt reduction in the total emission intensity is observed with increasing the well width (inset of Fig. 2). In the figure, the emission intensity was evaluated by the spectral integration of the quantum well emission band at the same excitation power. The accuracy is approximately $\pm 10\%$. Even though the integrated emission intensity of the PL is not strictly proportional to the oscillator strength (as it is influenced by the nonradiative recombina-

TABLE I. Material parameters used in the calculations.

	GaN	AlN
E_g (eV)	3.51	5.1
m_e (m_0 units)	0.3	
m_h (m_0 units)	1.55	
ϵ (relative)	10.4	10.4
e_{31} ($C\ m^{-2}$)	-0.49	-0.60
e_{33} ($C\ m^{-2}$)	0.73	1.46
C_{13} ($10^{11}\ dy/cm^2$)	10.8	12
C_{33} ($10^{11}\ dy/cm^2$)	39.9	39.5
a (Angstrom)	3.189	3.11

tion processes, which are assumed to be constant in all samples at first order), these results indicate a clear well width dependence. In fact, no quantum well emission could be measured from the 9 nm samples under excitation power and alignment conditions identical to those of the other samples.

IV. THEORETICAL RESULTS AND DISCUSSION

In what follows, we attempt a quantitative analysis of our data, taking into account all the possible contributions to the built-in field in the structure. The built-in electric field originates by the accumulation of a polarization charge at the interfaces of GaN/Al_{0.15}Ga_{0.85}N heterostructures. The total polarization charge can be written as $P_{tot} = P_{piezo} + P_{spont}$, where P_{piezo} is the piezoelectric charge caused by the lattice mismatch (mis) and by the thermal strain (ts) [$P_{piezo} = P_{mis} + P_{ts}$], whereas P_{spont} represents the spontaneous polarizability of the GaN/Al_{0.15}Ga_{0.85}N interface, as clearly demonstrated by the recent works of Bernardini *et al.*⁷⁻⁹ For an alternating sequence of wells (w) and barriers (b) the total electric field in the well can be calculated as⁹

$$F_w = L_b(P_{tot}^b P_{tot}^w) / [\epsilon_0(L_w \epsilon_b + L_b \epsilon_w)], \quad (1)$$

$\epsilon_{b,w}$ being the relative dielectric constant of the layers (analogous expression with exchanged indexes holds for the electric field in the barrier). The piezoelectric charge induced by the lattice in-plane mismatch ($\sigma_{||}$) can be calculated as $P_{lm} = -2(e_{33}C_{11}/C_{33} - e_{31})\sigma_{||}$, where e_{ij} and C_{ij} are the piezoelectric tensor components and the elastic constants, respectively, as given in Refs. 1, 2, and 7-9 and Table I. Since, the layers are grown on thick GaN buffer layers, we expect that the GaN quantum wells are relaxed and take the bulk GaN lattice constant of the buffer (3.189 Å). Moreover, we assume that the Al_{0.15}Ga_{0.85}N layers grow pseudomorphically in our structures and undergo a tensile in-plane strain $\sigma_{||} = 0.37\%$. The assumption of a strained Al_{0.15}Ga_{0.85}N barrier is consistent with the observation of pseudomorphic growth of Al_{0.15}Ga_{0.85}N layers for thicknesses as large as hundreds of nm,² which is much thicker than the total amount of Al_{0.15}Ga_{0.85}N contained in our 10 periods multiple quantum wells, and with the findings of Ref. 6. This results in a piezoelectric polarization charge $P_{lm}^w = 0$ in the quantum well and $P_{lm}^b = -0.0070\ C/m^2$ in the Al_{0.15}Ga_{0.85}N barrier. On the other hand, the thermal strain in our experimental conditions amounts to some 0.003%, resulting in an addi-

tional polarization charge of the order of $P_{ts}^w = -3.2 \times 10^{-4}\ C/m^2$. As far as the spontaneous polarization charge is concerned, we take the recent data of Refs. 7-9, leading to $P_{sp}^w = -0.029\ C/m^2$ and $P_{sp}^b = -0.037\ C/m^2$, the latter value being obtained by linear interpolation of the GaN and AlN values ($P_{sp} = -0.08\ C/m^2$ in AlN). By using these data and Eq. (1) we can calculate the built-in field in the different samples, which turns out to vary in the range 0.8-1.3 MV/cm depending on the actual well width.

At first order, neglecting high-field effects and corrections for free-charge screening, we might expect that the built-in field causes a redshift of the quantum well gap given by the quadratic Stark effect.¹⁰⁻¹¹ However, such an approximation is too simplistic and actually reproduces only qualitatively the field dependence of the redshift. A full treatment of the data must go beyond the perturbation theory and requires a full solution of Schrodinger and Poisson equations, especially in the presence of injected carriers that screen the internal field. On the other hand, the presence of high electric fields and the peculiar band structure of wurtzite semiconductors limit the applicability of the usual effective mass approaches. To overcome such limitations and to treat the problem non-perturbatively, a self-consistent tight-binding (TB) model should be used.¹² The tight-binding model is used to describe the electronic structure in the entire Brillouin zone, up to several eV above the fundamental gap. For the specific case of nitrides, the parameters of our empirical TB model were determined by fitting the density-functional theory local-density approximation (DFT-LDA) bandstructure as outlined in Ref. 12. For the self-consistent calculations the electron and hole quasi-Fermi levels are calculated for a given photoinjected charge density. The resulting electron and hole distribution functions (n and p , respectively) are used to solve the Poisson equation

$$\frac{d}{dz}D = \frac{d}{dz} \left(-\epsilon \frac{d}{dz}V + P_{tot} \right) = e(p - n), \quad (2)$$

where D and V are the displacement field and the potential, and P_{tot} is the total polarization charge discussed above. The obtained potential is thus inserted into the TB Schrodinger equation which is solved to get the energies and wave functions. The new quasi-Fermi levels are thus recalculated and the procedure is iterated until self consistency is achieved. The results of the self-consistent calculations are shown by the solid curves in Fig. 2 (both for the energy of the E_{1e1h} emission and for the oscillator strength in the inset). The agreement with the experimental data is very good both for the trend and for the absolute values. The effect of screening is clearly observed in the progressive blueshift of the eigenstates occurring with increasing the injected carrier density. For the present experimental conditions, we expect that the photogenerated carrier density is around $10^{12}\ cm^{-2}$. The neglect of the spontaneous polarization field in the self-consistent calculations indeed results in the dashed curve of Fig. 2, which is quite far from the measured values (this curve was obtained in the low-density limit $n = 1 \times 10^{11}\ cm^{-2}$. Even larger values would be obtained assuming $n > 1 \times 10^{11}\ cm^{-2}$). These results clearly indicate the importance of the spontaneous polarization field and of the

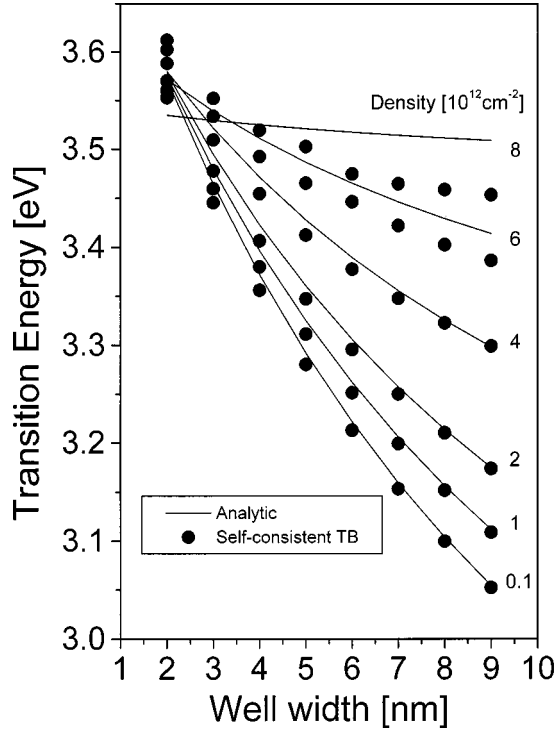


FIG. 3. Comparison between the analytic expression Eq. (4) (solid lines) and self-consistent tight-binding results (solid circles).

self-consistent treatment of the electronic states of Nitride-based quantum wells, also in view of the design of optoelectronic devices. To this aim, a simplified method can be developed to approximately reproduce the effects of the internal field and of the screening forecast by the calculations. Namely, (i) the rectangular quantum well is replaced by a triangular well resulting from the total built-in field, and (ii) the two-dimensional (2D) photo injected charge density (σ) is considered to accumulate at the GaN/Al_{0.15}Ga_{0.85}N interface. With these approximations the electric field in the well becomes

$$F_w = L_b(\sigma + P_{\text{tot}}^b - P_{\text{tot}}^w)/[\epsilon_0(L_w\epsilon_b + L_b\epsilon_w)] \quad (3)$$

and

$$E_{1e1h} = E_g - F_w L_w + \left(\frac{9\pi\hbar e F_w}{8\sqrt{2}} \right)^{2/3} \left(\frac{1}{m_e} + \frac{1}{m_h} \right)^{1/3}. \quad (4)$$

The comparison between the analytic formula Eq. (4) and the self-consistent tight-binding results is shown in Fig. 3 for several injected charge density. All the parameters used to evaluate Eqs. (3) and (4) are taken from the literature^{7-9,12-14} (see Table I). The parameters for Al_{0.15}Ga_{0.85}N are obtained by linear interpolation of the AlN and GaN ones. The analytic results reproduce quite well the TB results for densities below $4 \times 10^{12} \text{ cm}^{-2}$. At higher density the spatial distribution of the injected charges should be taken into account properly for a quantitative analysis (indeed under this condition one cannot assume that charges simply accumulate at the GaN/Al_{0.15}Ga_{0.85}N interfaces). From Fig. 3 we also notice that the agreement between Eq. (4) and TB results improves as the well width increases. In fact, for narrow wells the triangular barrier approximation is no longer valid. The

neglect of the triangular well term (last term) in Eq. (4), in fact results in the overestimate of the Stark shift by approximately 300 meV in narrow wells and 100 meV in wide wells. In conclusion we can say that Eq. (4) can be used for the design and the analysis of GaN-based heterostructures and devices as soon as the well width is larger than 2 nm and the density of injected carriers is below $4 \times 10^{12} \text{ cm}^{-2}$.

So far, we have demonstrated that the main consequences of the QCSE is the shift of the eigenstates and the reduction of the oscillator strength of the transitions. However, the comparison between theory and experiments shown in Fig. 2 has been performed in a pure single-particle picture, in which the exciton binding energy has been neglected. This point is quite interesting since one might expect two competing effects to occur in GaN quantum wells: namely, (i) the enhancement of the exciton binding energy caused by the quantum confinement, and (ii) the reduction of the exciton binding energy caused by the decreased wave-function overlap induced by the internal field. Since it is not *a priori* clear which one of the two effects is dominant, it is crucial to perform a detailed calculation of the exciton binding energy in GaN quantum wells, taking into account the built-in field. As a matter of comparison, we know from the II-VI Zn_xCd_{1-x}Se/ZnSe quantum wells that the exciton binding energy ranges around 30–40 meV for typical well widths of 3–4 nm and Cd content of approximately 0.2–0.3. In this material system, we have already shown experimentally and theoretically¹⁵ that the exciton oscillator strength and binding energies are dramatically reduced by electric fields well below 100 kV/cm. By analogy, we thus expect that the strength of the built-in field (MV/cm) can seriously affect the exciton stability of GaN quantum wells. To quantify the problem, we have evaluated the well width dependence of the exciton binding energy in our quantum wells exploiting our recent Green's-function model¹⁶ and using the self-consistent tight-binding wave functions discussed above. These are inserted in the form factor

$$F(q) = \int dz_e \int dz_h |\chi_e(z_e)|^2 |\chi_h(z_h)|^2 e^{-q|z_e - z_h|}, \quad (5)$$

which is computed numerically [$\chi_{e,h}(z)$ are the wave functions of the electron and the hole along the growth axis]. Due to the lack of experimental absorption or photoluminescence excitation data on nitride-based quantum wells showing clear exciton resonances, the model was preliminarily tested on Zn_xCd_{1-x}Se/ZnSe quantum wells,¹⁵ giving results for the exciton binding energy and oscillator strength in excellent agreement with the experimental data. In Fig. 4(a), we plot the well width dependence of the exciton binding energy in our GaN/Al_{0.15}Ga_{0.85}N quantum wells, in the flat band case (squares) and with the inclusion of the built-in field (dots). Neglecting the built-in field one would expect exciton binding energies much larger than the bulk value, in the investigated well width range. However, the separation of the wave functions induced by the built-in field strongly reduces the binding energy, which becomes as low as 10 meV in a 5 nm-thick well. Therefore, we find that despite the strong polarity of the nitride quantum wells, which should lead to a very strong exciton binding energy, the existence of an internal field in these heterostructures reduces the exciton binding energy to values comparable to those measured in

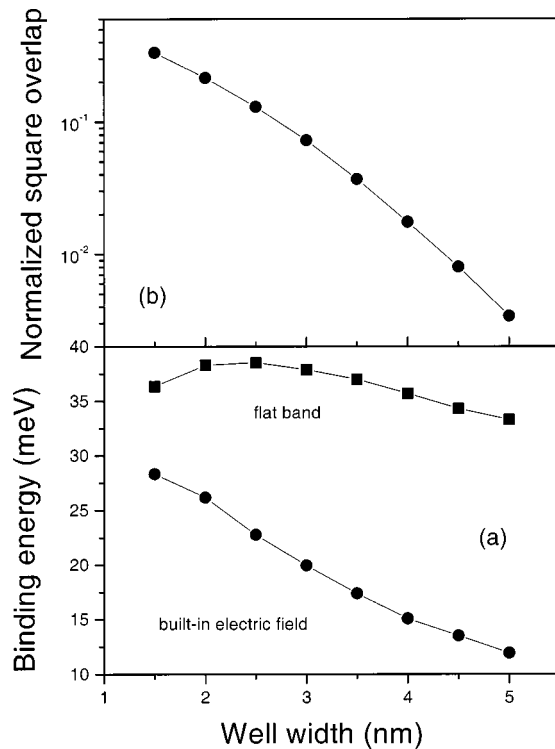


FIG. 4. Well-width dependence of the exciton binding energy calculated in the tight-binding model (dots) and in the flat-bands case (squares). Inset: square overlap integral of the electron and hole wave functions normalized to the flat-band case.

narrow-gap III-V heterostructures (namely GaAs/Al_{0.15}Ga_{0.85}As).

Finally, in Fig. 4(b) we have calculated the well width dependence of the square overlap of the wave functions, by using the tight-binding model. The results show that the square overlap normalized to the flat band case varies between about 0.2 for the 2 nm well and 10^{-3} for the 5 nm

well. The expectation of a small oscillator strength together with a reduced binding energy suggest that excitons cannot be easily measured in optical spectra of nitride quantum wells, especially at high temperature or in the presence of strong disorder-induced broadening. To the best of our knowledge, despite the large number of reports on the optical properties of nitride-based quantum wells, we are indeed not aware of any spectroscopic study in which sharp excitonic resonances have been observed in the luminescence excitation or transmission spectra of GaN and In_xGa_{1-x}N quantum wells. Moreover, excitons can be safely neglected in the comparison between the PL data and the single-particle transition energies shown in Fig. 2.

V. CONCLUSIONS

In conclusions, we have shown that the optical properties of GaN/Al_xGa_{1-x}N quantum wells are strongly affected by the built-in electric field originated by the spontaneous polarization charge, and, to a minor extent, by strain. The well width dependence of the fundamental $1e-1h$ transition is quantitatively explained by means of a self-consistent tight-binding model accounting for screening (either dielectric and of free carriers) and for the spontaneous polarization charge existing at the GaN/Al_{0.15}Ga_{0.85}N interfaces. The binding energy and the oscillator strength of the exciton are both found to reduce substantially due the presence of the built-in field.

ACKNOWLEDGMENTS

One of the authors (R.C.) gratefully acknowledges Virginia Commonwealth University for the hospitality. This work is partially sponsored by INFN-Italia through Progetto Sud, by 40% MURST, by European Community Network ULTRAFast and by the Office of Naval Research and Air Force Office of Scientific Research. We are indebted to A. Rizzi, V. Fiorentini, and F. Bernardini for helpful discussions.

*Permanent address: Istituto Nazionale Fisica della Materia (INFN), Dipartimento Ingegneria dell'Innovazione, University of Lecce, Lecce, Italy.

[†]Present address: National Research Council, Institute for Microstructural Sciences, Ottawa, Ontario, Canada K1A 0R6.

[‡]Present address: Emory University, Department of Physics, Atlanta, GA 30303.

[§]Permanent address: CNR-IME Istituto per lo studio di nuovi Materiali per l'Elettronica, Via per Arnesano, I-73100 Lecce, Italy.

¹T. Takeuchi, C. Wetzel, S. Yamaguchi, H. Sakai, H. Amano, I. Akasaki, Y. Kaneko, S. Nakagawa, Y. Yamaoka, and N. Yamada, *Appl. Phys. Lett.* **73**, 1691 (1998).

²T. Takeuchi, S. Sota, M. Katsuragawa, M. Komori, H. Takeuchi, H. Amano, and I. Akasaki, *Jpn. J. Appl. Phys., Part 2* **36**, L382 (1997).

³S. H. Park and S. L. Chuang, *Appl. Phys. Lett.* **72**, 3103 (1998).

⁴J. S. Im, H. Kollmer, J. Off, A. Sohmer, F. Scholz, and A. Hangleiter, *Phys. Rev. B* **57**, R9435 (1998).

⁵A. Bykhovski, B. Gelmont, and M. Shur, *Appl. Phys. Lett.* **63**, 2243 (1993).

⁶M. Leroux, N. Grandjean, M. Laugt, J. Massies, B. Gil, P. Lefebvre, and P. Bigenwald, *Phys. Rev. B* **58**, R13 371 (1998).

⁷F. Bernardini, V. Fiorentini, and D. Vanderbilt, *Phys. Rev. B* **56**, R10 024 (1997).

⁸F. Bernardini, V. Fiorentini, and D. Vanderbilt, *Phys. Rev. Lett.* **79**, 3958 (1997).

⁹F. Bernardini and V. Fiorentini, *Phys. Rev. B* **57**, R9427 (1998).

¹⁰G. Bastard, in *Wave Mechanics Applied to Semiconductor Heterostructures* (Edition de Physique, Paris, France, 1987).

¹¹J. Singh, *Semiconductor Optoelectronics* (McGraw Hill, New York, 1995).

¹²A. Di Carlo, S. Pescetelli, M. Paciotti, P. Lugli, and M. Graf, *Solid State Commun.* **98**, 803 (1996); F. Della Sala, A. Di Carlo, P. Lugli, F. Bernardini, V. Fiorentini, R. Scholz, and J. M. Jancu, *Appl. Phys. Lett.* **74**, 2002 (1999).

¹³S. Nakamura and G. Fasol, *The Blue Laser Diode* (Springer-Verlag, Berlin, 1997).

¹⁴D. Vogel, P. Krügel, and J. Pollmann, *Phys. Rev. B* **55**, 12 836 (1997).

¹⁵P. V. Giugno, M. DeVittorio, R. Rinaldi, R. Cingolani, L. Vanzetti, L. Sorba, and A. Franciosi, *Phys. Rev. B* **54**, 16 934 (1996).

¹⁶G. Traetta, G. Coli, and R. Cingolani, *Phys. Rev. B* **59**, 13 196 (1999).